Jón Andri Árnason*, Ragnhildur Guðmundsdóttir-Korchai, Yonatan Afework Tesfahunegn and Þórður Helgason,

Novelle approach to simulating spinal cord stimulation during tSCS using CT images and FEM

https://doi.org/10.1515/cdbme-2024-2009

Abstract: Transcutaneous spinal cord stimulation (tSCS) offers non-invasive relief for chronic pain and improves motor function in spinal cord injured (SCI) patients. However, its mechanisms are not currently fully understood, and patient-specific factors, such as Body mass index (BMI) and age, complicate treatments. This paper aims to understand tSCS better by developing a novel Finite Element Model (FEM) of the human body using CT scans. Three subjects (sex, male, female, male. Age: 26, 27, 64. BMI: 38.9, 24.1, 28.4) underwent a CT scan, performed on a Cannon Aquilion Prime (Slice thickness [mm]: 0.8, Voxel size [mm^3]: 0.564, 0.328, 0.527), which imaged the trunk of the body, from top of the abdomen to the bottom of the pelvis. The images were then used in Materialize Mimics Research 21.0 to create 3D images of individual organs, skin, fat, muscles, skeleton, and spinal cord. After pre-processing in Autodesk Meshmixer, the models were converted into solid CAD objects in Ansys SpaceClaim R2021 and combined into a single abdominal model. Ansys Maxwell R2021 was then used for simulations. Five different two-electrode configurations were tested in the prototype phase with a simplified model setup. The positive electrodes were placed over the (Thoracic) T10, T12, (Lumbar) L2 and L4 vertebrae sequentially, with the negative electrode over (Sacral) S2. The simulations took on average 47.4 hours. A marked decline in electrical current penetration depth was observed as the electrodes were placed closer together which was consistent with known current distribution patterns. A preliminary validation test was also performed using a lamb's thigh. Two electrodes were placed a known distance apart and a stimulation was given, needle electrodes were then inserted in a grid-like pattern to obtain voltage values. The setup was recreated and simulated in Ansys Maxwell. The resulting average percent difference was 44.93 ± 33.3 % (5Vpp Square wave) and 35.02 ± 23.38 % (5V DC). In both instances, the highest difference was at the edges of the electrodes and the lowest difference in the midpoint between electrodes. Later versions of FEM models incorporated more organs and had improved on previous mesh generation flaws, but encountered new mesh generation errors which could not be rectified before the conclusion of the master's project. Despite complications, this project has provided a pipeline for creating similar models and shown their usability. Future work will involve overcoming the current mesh generation errors, reducing calculation time, and performing a thorough validation test.

Keywords: tSCS, CT, FEM

1 Introduction

Transcutaneous spinal cord stimulation (tSCS) stands as a promising non-invasive therapy for chronic pain management and motor function enhancement among individuals suffering from spinal cord injuries (SCI)[1]. tSCS involves placing electrodes on the surface of the skin and stimulating with electrical current to activate the underlying neural circuitry [2]. However, this surface-based approach presents challenges in accurately targeting the region of interest (ROI) due to factors such as electrode placement, shape, current intensity, and patient-specific physical characteristics influencing current distribution. To overcome these limitations, finite element modelling (FEM) has emerged as a powerful tool for simulating electric current distribution in the human body [3]. Leveraging mathematical algorithms, FEM discretizes complex structures into smaller elements for accurate analysis of electric field behaviour.

***Corresponding author: Jón Andri Árnason:** Reykjavík University, Menntavegur 1, Reykjavík, Iceland, ajonandri@gmail.com.
2nd Author Ragnhildur Guðmundsdóttir-Korchai, 3rd Author Yonatan Afework Tesfahunegn, 4th Author Þórður Helgason: Reykjavík University, Reykjavík, Iceland.

2 Methods

2.1 Model creation pipeline

The creation process began with a set of CT images obtained from 3 subjects (sex, male, female, male. Age: 26, 27, 64. BMI: 38.9, 24.1, 28.4).

The CT images were imported into Materialize Mimics where a 3D model was created for each organ. A simple mask is created using the HU value thresholds (upper and lower) for the desired organ. Manual manipulation of the mask is then performed with the assistance of interpolation algorithms to overlay the mask accurately over the organ. Only the outer boundary of the organ needs to be replicated as the internals will be solid. The mask is then converted into a 3D STL model and exported for post-processing in Autodesk Meshmixer. The post processing involved closing any unwanted holes, removing any internal geometry and smoothing rough edges. The models were then inspected for any errors generated during the process and exported as a new STL version. The organ STL models were then imported into Ansys SpaceClaim.

In Ansys SpaceClaim the facets of the model were regularized with a shrink wrap function to around 1 mm in edge length. Once the facets were regularized and error free the different organ models would be opened in a single project to ensure that no overlap occurred on the boundaries, models

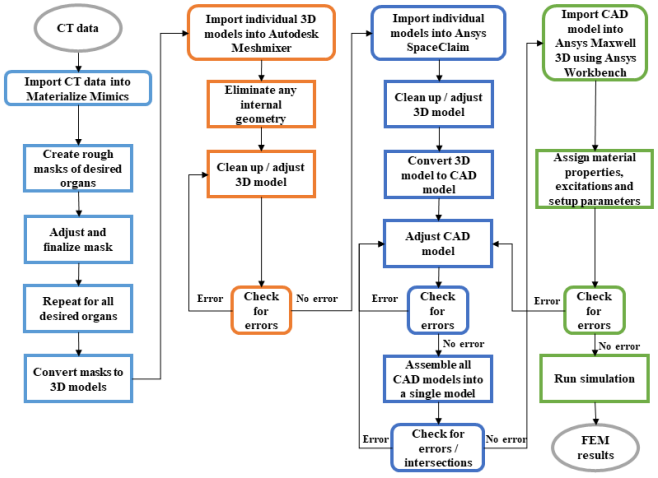

Figure 1: Model creation pipeline.

could share the same physical space if the outer geometry was not in contact with another organ model. Once the organ models have been checked for intersections and the facets regularized the purely geometrical STL models were converted into solid CAD objects more suitable for calculations.

After conversion the separate organ models were once more imported into a single project. Next the electrodes were introduced to the model by drawing the desired electrode shape in a work plane above the skin model, then dragging the outline partially through the skin, then removing the overlapping areas from the electrode to create an electrode that contacts the skin model at all points. The combined model can then be imported into Ansys Maxwell using Ansys workbench R2021 for simulations.

Table 1: Biological tissue electrical specific conductivity according to five different publications. Since each value is different depending on the source the average was taken and used for the simulations. x denotes no value obtained from source.

Material	Specific conductivity [S/m]					Values used [S/m]
Blood	0.7	0.63	0.66	0.6	0.68	0.65
Cortical bone	0	0.01	0.01	x	0.06	0.022
Fat	0	0.04	0.08	0	0.05	0.047
Heart	0.1	x	0.39	0.3	0.28	0.28
Kidney	0.1	x	0.34	0.6	0.45	0.37
Liver	0.1	x	0.19	0.1	0.17	0.13
Lung	0.1	x	0.1	0.1	x	0.099
Muscle	0.4	0.01	0.46	0.1	0.34	0.45
Spinal cord	0.3	x	0.61	x	0.45	0.45
Skin	0.1	0.44	0.15	x	x	0.23
Stomach	0.5	x	0.16	x	x	0.33
Source:	[4]	[5]	[6]	[7]	[8]	

In Maxwell, each organ model is given a conductivity value (See Table 1). Then the desired excitation is given to the electrodes, current flowing into the model at the positive electrode and out at the negative. The model was then ready for simulations.

2.2 Prototype model

Early in the project a prototype was made with the CT scans from subject 1 to test the feasibility of the pipeline. It involved models of the skin, fat, muscle, bones and spinal cord. Once assembled according to the pipeline the composite model was cut into a rectangular shape centred on the spinal cord to reduce the calculation time. Two 5 cm circular electrodes were created and placed above the T10, T12, L2, L4 and S2 spinal vertebrae. The S2 electrode was negative and remained fixed, the other electrodes were positive and were placed one at a

time and simulated. One simulation also contained all previous electrodes with only the T10 and S2 active. The excitation was set to 10 mA entering and exiting the system. Each tissue was given a value according to table 1.

2.3 Preliminary validation test

Validation is one of the most important aspects of any simulation research, however attempting to measure the electrical currents inside a living human body at multiple points is a difficult process, therefore a simpler method was devised using a lambs thigh. Two 5 cm diameter StimTrode Neurostimulation electrodes were placed on bare muscle tissue, 9 cm apart. A Neuroline inoject needle electrode was then inserted into the thigh at specific points to create a grid. The needle was inserted at 5 different depths: 1, 12.5, 25, 37.5, 50 mm. This test was performed once using a 10 Hz, 5 V_{pp} square wave and again using 5V, 0,01 A DC current. Due to high activity in the hospital used for previous CT scans, a CT scan for the lambs thigh could not be performed. The lambs thigh was thus recreated in Ansys SpaceClaim with the use of images from all angles, then simulated in Ansys Maxwell using the same excitations. The percent difference between obtained and simulated voltage values was then calculated.

3 Results

3.1 Model creation

The first iteration of the pipeline process focused too much on model accuracy when creating in Materialize Mimics which resulted in longer creation time and increased error rate further down the pipeline. This was remedied by relaxing the requirements and using wrapping functions in Ansys SpaceClaim to fix small holes and mesh errors. The difference in creation approach can be seen in the muscle model of subject 1 and 3 (See figure 4). The next iteration, where the models for subjects 2 and 3 were created allowed for more loss in geometric accuracy in exchange for quicker creation time. This also had the added benefit of reduced simulation time as the geometry that needed to be computed in Maxwell was not as complex.

After the prototype model simulation mentioned in chapter 2.2 and 3.2 the simulations would run into an error where the simulation would complete with large parts of the mesh not being generated for multiple organs. This type of error could not be remedied before the completion of this project, but the partial completion of the simulation is a strong indicator for the methods possibilities.

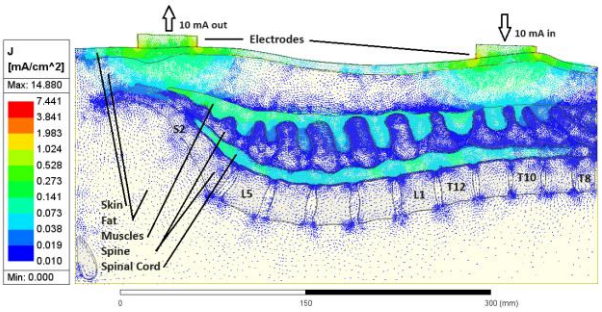

Figure 2: 5 mm cross section simulation results with a point cloud view of the T10 to S2 prototype configuration. Point density and color denotes the density of current in each area. 10 mA current enters the right electrode and exits through the left. Results are logarithmic. The edges of the electrodes predictably have the highest density which spreads out mostly through the shortest path, the skin, and down into the lower structures. The muscles and spinal cord have higher specific conductivity and thus have a preferably higher current density than the surrounding structures.

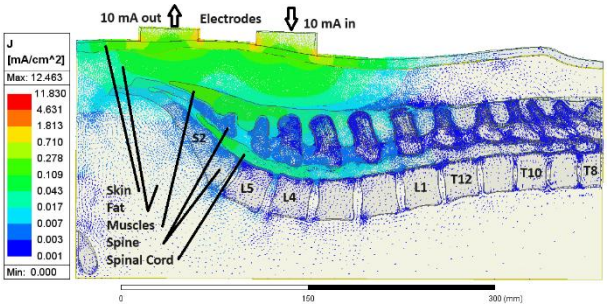

Figure 3: 5 mm cross section simulation results with a point cloud view of the L4 to S2 prototype configuration. With the electrodes closer the distribution pattern of the electrical current changes dramatically, much less total current reaches the spinal cord with the areas of strongest stimulation being directly between the two electrodes.

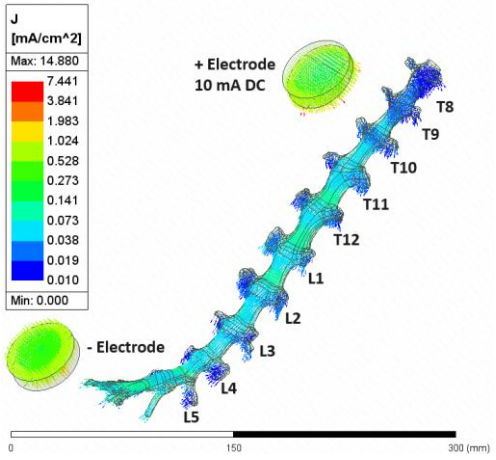

Figure 4: Isolated view of the spinal cord and the two electrodes with a vector view of the T10 to S2 prototype configuration. The color denotes the current density at each point and the direction of the arrow shows the path of the current. With this view can be seent how the current travels along the spinal cord and orthagonal to the exiting nerves at the vertebral exits. Due to not enough contrast between the soft materials this spinal cord model more closelly resembles the spinal canal than the spinal cord lacking the cauda equina.

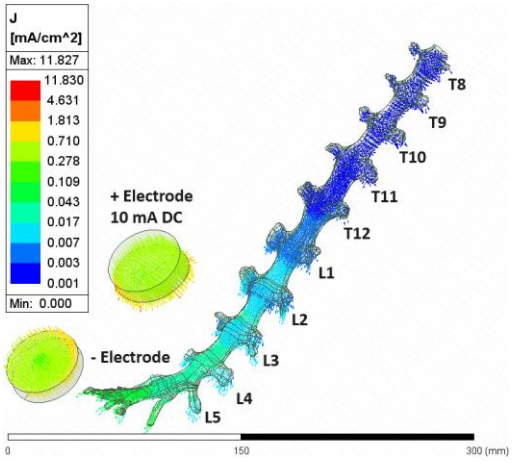

Figure 5: Isolated view of the spinal cord and the two electrodes with a vector view of the L4 to S2 prototype configuration. Here the affect of electrode positioning can be seen more clearly. The current is more targeted between the electrodes but has a much lower penetration depth, highlighting the problems faced with current tSCS therapies as higher accuracy typically means lower delivered current. Therefore carefully placing the electrodes according the the patients body structure is crucial and can guided by simulations.

Table 2: Simulation completion time using the following PC: windows 11, AMD Ryzen 5 5600X 6-core 4.20 GHz, 64 GB Corsair Vengeance DDR 4 3200 MHZ, GeForce RTX 3070 8GB.

Calculation time:	**Hours**
T10 to S2	48,3
T12 to S2	45,7
L2 to S2	52,2
L4 to S2	50,7
T10 to S2 + 3E	40,2
Average:	47,42
Deviation	4,23

3.2 Prototype model

The prototype models simulated successfully albeit with a high simulation time and poor mesh quality. The simulation time (see Table 2) was on average 47.42 ± 4.2 hours. With the mesh tending to clump together in very high densities around the border of each face of the solid CAD models resulting in a higher simulation time and an expected lower accuracy.

Table 3: Current density point results from the center of the spinal cord at each vertebral nerve exit. The T10 to S2 + 3E configuration contains three inactive electrodes on the surface of the skin, providing a pathway of lower resistance across the skin, this reduces the total current density amount as compared to the T10 to S2 configuration. This reveals a potential concern for multi-electrode setups.

[mA/cm^2]	**T10S2**	**T12S2**	**L2S2**	**L4S2**	**T10S2 + 3E**
T8	0,009	0,003	0,001	0,000	0,008
T9	0,020	0,006	0,001	0,000	0,017
T10	0,033	0,011	0,002	0,000	0,028
T11	0,041	0,018	0,004	0,001	0,036
T12	0,051	0,033	0,010	0,003	0,045
L1	0,047	0,038	0,016	0,005	0,042
L2	0,042	0,037	0,023	0,007	0,038
L3	0,042	0,039	0,029	0,011	0,038
L4	0,049	0,046	0,040	0,019	0,046
L5	0,068	0,065	0,058	0,030	0,064

The simulated results however matched the current understanding of electrical current distribution inside the human body as the current spread throughout the volume conductor model with much of the current travelling along the skin and upper areas. Some current passes through the fat, muscle and in between the vertebrae to reach the spinal cord (see figures 2 and 3), which has a higher specific conductivity value and thus is the path of least resistance for the local current. Moving the positive electrode towards the negative without changing the excitation current both lowers the total amount of current that reaches the spinal cord as well as what areas of the spinal cord are stimulated.

Additionally placing virtual point in the centre of the spinal cord at each vertebral nerve exit further showed the drop in electrical current penetration depth with increasing proximity between the electrodes (see Table 3).

These prototype results also show that indeed the electrode positioning can be used to direct the flow of electric current. Opening the doors for individualized therapies based on the structure of each patients bodies and simulated to find the most likely areas to stimulate the desired regions of the spinal cord, however more research and further improvements on the models is required before such therapies can be performed.

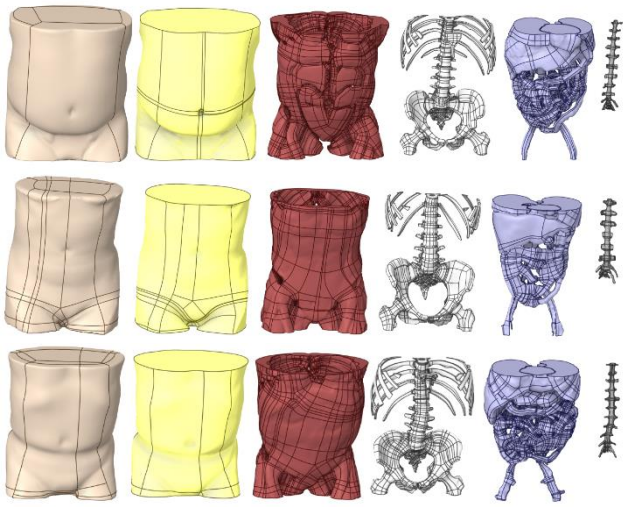

Figure 6: Seperated view of completed CAD models. Top is subject 1, middle is subject 2 and bottom is subject 3. Left most object is the skin model which surrounds the fat model. Second left is the fat model which envelopes all other models and is a conducting medium between two or more models not in direct contact. Middle two models are the muscle and skeleton models respectivelly. Second to right is an aggregation of internal organs (lungs, heart, liver, stomach, intestines, major bloodvessels). Right most object is the spinal cord model. The exact position of each organ model was preserved by not moving the organs from the origin point during the creation process, ensuring accurate biological positioning.

3.3 Preliminary validation test

Results showed a 44.93 ± 33.3 % difference between obtained and simulated results for the square wave test and a 35.02 ± 23.38 % difference for the DC test. The lowest difference was in the centre between the electrodes and the highest difference at the edges of the electrodes, indicating a layer of high resistance at the electrode to muscle interface that needs to be accounted for during simulations.

4 Conclusion

The pipeline has shown promise in simulating the human body during the tSCS process. While currently time-consuming to create each model has a high geometric accuracy and is capable of simulating nearly every tSCS electrode configuration. The simulations themselves, performed in Ansys Maxwell as also currently time-consuming but deliver a clear map of current distribution throughout the patient's body. Current iterations of the models are limited by a meshing error but have been proven viable in the prototype phase.

Preliminary validation tests, using lamb's thigh and needle electrodes have also shown have also shown a percent difference within believable ranges which are a target of improvement for future work.

Other future work includes solving the meshing error, reducing the calculation time, and performing a proper validation test.

Author Statement

Research funding: This research was partially funded by the Icelandic Centre for Research, Rannís. Additionally organizational assistance and access to medical equipment was provided by the rehabilitation division of the National University hospital of Iceland, Grensás.

Conflict of interest: Authors state no conflict of interest. Informed consent: Informed consent has been obtained from all individuals included in this study. Ethical approval: The research related to human use complies with all the relevant national regulations, institutional policies and was performed in accordance with the tenets of the Helsinki Declaration, and has been approved by the authors' institutional review board or equivalent committee.

References

[1] C. Norrbrink, “Transcutaneous electrical nerve stimulation for treatment of spinal cord injury neuropathic pain.”, Journal of rehabilitation research and development, vol. 46, no. 1, 2009.

[2] K. Minassian, I. Persy, F. Rattay, M. R. Dimitrijevic, C. Hofer, and H. Kern, “Posterior root-muscle preflexes elicited by transcutaneous stimulation of the human lumbosacral cord”, Muscle and Nerve, vol. 35, no. 3, 2007.

[3] A. Opitz, W. Legon, A. Rowlands, W. K. Bickel, W. Paulus, and W. J. Tyler, “Physiological observations validate finite element models for estimating subject-specific electric field distributions induced by transcranial magnetic stimulation of the human motor cortex”, NeuroImage, vol. 81, 2013.

[4] A. Hirata, Y. Takano, Y. Kamimura, and O. Fujiwara, “Effect of the averaging volume and algorithm on the in situ electric field for uniform electric- and magnetic-field exposures”, Physics in Medicine and Biology, vol. 55, no. 9, 2010.

[5] C. Ramon, P. Garguilo, E. A. Fridgeirsson, and J. Haueisen, “Changes in scalp potentials and spatial smoothing effects of inclusion of dura layer in human head models for EEG simulations”, Frontiers in Neuroengineering, vol. 7, 2014.

[6] Low Frequency (Conductivity) » IT’IS Foundation. [Online]. Available: https://itis.swiss/virtual-population/tissue-properties/database/low-frequency-conductivity/

[7] D. Miklavčič, N. Pavšelj, and F. X. Hart, “Electric Properties of Tissues”, in Wiley Encyclopedia of Biomedical Engineering, 2006.

[8] K. Meyer-Waarden, “Bioelektrische Signale und ihre Ableitverfahren”, in Stuttgard: Schattauer, 1985.